ELECTRON CLOUD SIMULATIONS FOR THE MAIN RING OF J-PARC

B. Yee-Rendon*, R. Muto, K. Ohmi, K. Satou, M. Tomizawa and T. Toyama

KEK/J-PARC, Tsukuba, Ibaraki, Japan

Abstract

The simulation of beam instabilities is a helpful tool to evaluate potential threats against the machine protection of the high intensity beams. At Main Ring (MR) of J-PARC, signals related to the electron cloud have been observed during the slow beam extraction mode. Hence, several studies were conducted to investigate the mechanism that produces it, the results confirmed a strong dependence of the beam intensity and the bunch structure in the formation of the electron cloud, however, the precise explanation of its trigger conditions remains incomplete. To shed light on the problem, electron cloud simulations were done using an updated version of the computational model developed from previous works at KEK. The code employed the signals of the measurements to reproduce the events seen during the surveys.

INTRODUCTION

In the past, several electron cloud simulations for the J-PARC MR were done to estimate the conditions of its formation and its effect in the beam stability [1–3]. In those cases, the longitudinal distributions used were bunched or coasting beams and the proton loss was the main source of primary electrons (seeds).

The MR accelerates protons up to energy of 30 GeV, it operates in two modes: Fast extraction (FX) and Slow extraction (SX) [4]. Electron cloud occurred during both modes. At FX, the phenomenon was mitigated by beam operation (scrubbing effect) [5]. On the contrary, the electron cloud remains at SX, therefore several surveys were done to investigate the conditions for its build-up [6,7]. It was observed that the electron cloud appeared during the debunching process, reaching the peak about 75 ms after P3 (the time when debunching starts). Indeed, the presence of a strong microbunch structure for the cases with electron cloud was also reported, thus, it is believed that this particular beam shape reinforce the electron multiplication. Finally, the low level of beam loss detected, before the electron cloud began to form, which indicates that residual gas ionization as the principal source of primary electrons.

Figure 1 presents a map of the electron cloud as a function of the beam intensity and phase difference at injection [7]. The work is focus to reproduce the electron cloud formation seen at SX, with emphasis in the cases of zero phase difference shown in Fig. 1. This study used the longitudinal beam distribution obtained by using a fast current transformer monitor and the pressure measured with vacuum gauges installed in the ring.

* byee@post.j-parc.jp
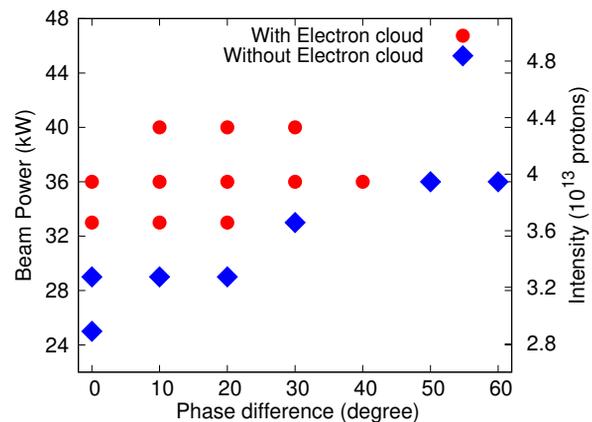
Figure 1: The presence (red circles) or absence (blue diamond) of the electron cloud as a function of the intensity and injection settings (phase difference between the beam and acceleration RF).

Additionally, the frequency spectrum of the electron cloud detector and the fast current transformer monitor in the electron cloud cases presented a large amplitude for the components between 20 to 40 MHz [6], which corresponds to the bouncing frequency of the electrons in the MR vacuum chamber [8]. Therefore, a sinusoidal distributions is employed to corroborate that the frequencies in the same range can increase the electron production in the simulations.

SIMULATION SETUP

The update model presented here includes new features such as the debunching process and the use of the data of the beam measurements as inputs. The simulation code is described elsewhere [1]. The relevant features of the model are:

- The longitudinal distribution and electrons are simulated by macro-particles. The beam profile is represented by 5231 macro-particles to describe the entire proton distribution around the ring (synchrotron period at the MR is 5.231 μs at 30 GeV).

- The effect of the microbunch structures is taking into account in the simulations. The beams distribution corresponded to a two different times in the debunching: 5 ms (the bunch has smooth shape) and 75 ms (the microwave structure in the beam is severe). Figure 2 shows the difference in the bunch shape for the same beam at these two times.

- CO and H_2 were used as the residual gas. Their ionization cross-section and the corresponding pressure, for the different intensities and times, are shown in Table 1.

- $\delta = 1.6$ and $E_{max} = 200\ eV$ were adopted for the Secondary Emission Yield (SEY) model. These parameters were based on the MR J-PARC beam pipes measurements [9].
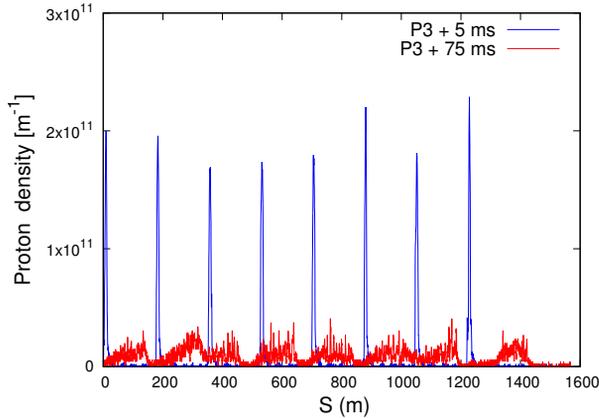
Figure 2: Longitudinal beam profile at two different times during the debunching process. A remarkable microbunch structure is presented at P3+75 ms.

Table 1: Simulations Parameters for the JPARC MR

Parameters	Units	Value
Energy	GeV	30
Bunch population[1]	$10^{13}ppp$	4.2, 3.8, 3.4, 2.8
Circumference	m	1567.5
Beam pipe radius	cm	6.5
rms bunch size	cm	0.5
Ionization cross section	$Mbarn$	2
Vacuum pressure at 5 ms[2]	μPa	0.2
Vacuum pressure at 75 ms[1] [2]	μPa	0.9, 0.7, 0.5, 0.4
Time step	ns	1

To verify if the simulations present a similar bouncing frequency as in the measurements, the model had the next changes:

- The longitudinal beam profile was a sinusoidal distribution "$A(I) \mid Sin(\pi f_0 t) \mid$", where $A(I)$ was a normalized factor such as the integration over all the circumference produced the corresponding intensity "I" for each case, and f_0 took values in a range from 10 to 100 MHz in an step of 10 MHz.
- The SEY model used $\delta = 1.1$ and $E_{max} = 200\ eV$.

RESULTS

Figure 3 shows an example of the longitudinal beam profile employed by our model (top) and its electron density generated (bottom) at 5 ms after P3. The largest amount of the secondary electron (electrons gained) after the bunch peak suggests the trailing edge multipactor is the main mechanism

---

[1] Each intensity has a corresponding vacuum pressure at 75 ms.
[2] The time after debunching starts (P3).

of secondary electron production. Each simulation case was repeated five times and the average value was reported with their corresponding standard errors (Figs. 4 and 6).
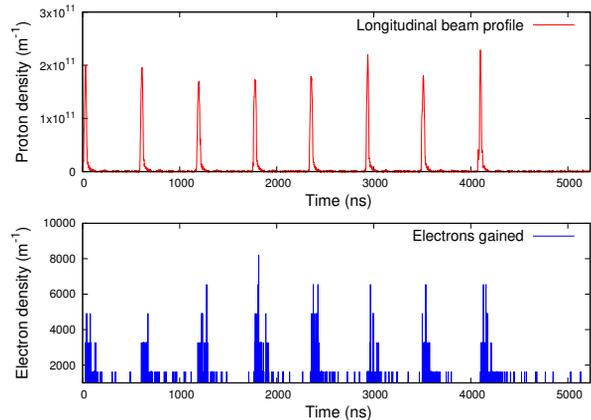
Figure 3: The longitudinal beam distribution (top) and the corresponding electron density (bottom). The data length corresponds to one turn of the J-PARC MR (5.231μs).

The summary for the simulations cases appears in Fig. 4. The numbers of electrons generated were similar for the cases using longitudinal beam distributions at 5 ms after debunching starts (Fig. 4 blue bars). In contrast, the results for the time of 75 ms presented a clear difference between the higher and lower intensities (Fig. 4 red bars). Indeed, the lowest intensity ($2.8\ x\ 10^{13}ppp$) produced almost the same amount of electrons for both times.
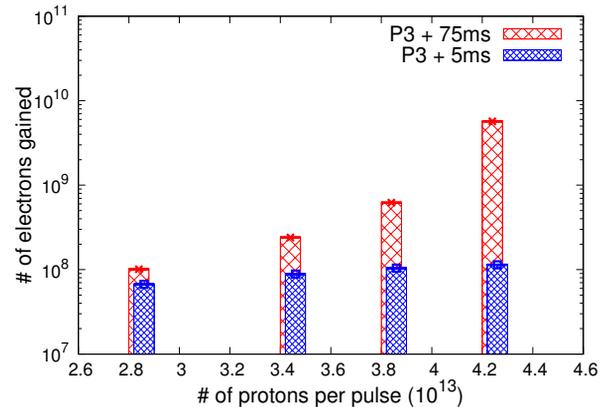
Figure 4: The comparison of the total electrons generated by the four intensities simulated at the two different times (5 ms and 75 ms after P3). The model used a $\delta = 1.6$ and $E_{max} = 200\ eV$.

Additionally, Fig. 5 presents the total flux charge measured by the electron cloud detector for the same cases as in the simulations. The charge flux per turn for the time of 5 ms was in the same range for all the cases (Fig. 5 blue bars). At 75 ms, an increase of the signal detected as a function of the intensity appeared. In addition, similar amounts of charge flux for the two time cases were observed in the lower intensities [7].
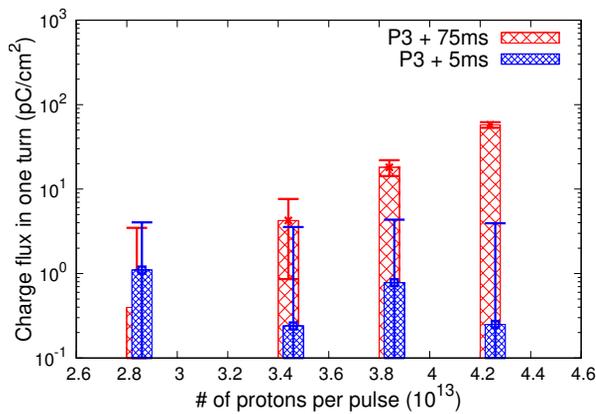
Figure 5: The total flux charge of the signal measured by the electron cloud detector in one turn. The signal was average over 100 turns, the beam fluctuations and detector noises are included in the error bars.

Finally, Fig. 6 shows the electrons gained as a function of the frequency of the sinusoidal distribution. A remarkable production of electrons were obtained at the high intensities for frequencies between 30 to 50 MHz. Due to the largest number of electron generated at certain frequencies δ was 1.1 for this study.
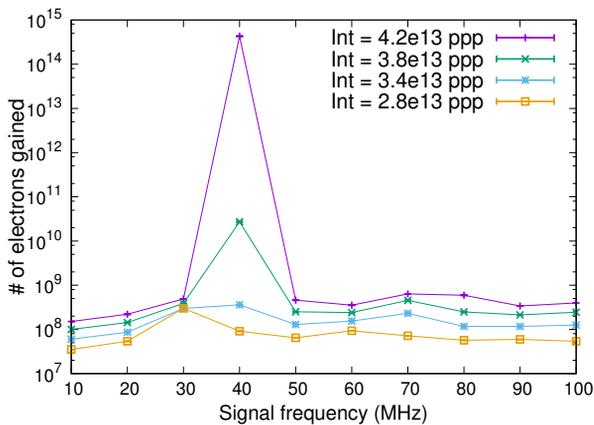
Figure 6: Electrons produced in the simulations vs. the frequency of the sine signal at different intensities, using $\delta = 1.1$ and $E_{max} = 200 \ eV$.

CONCLUSIONS

The map of Fig. 1 shows that for the first column (phase difference equal to zero degrees), the electron cloud did not appear in the lower intensities, on the contrary, it developed in the higher cases. The same conclusion can be obtained from the values presented in Figs. 4 and 5 using the next interpretation: at the beginning of debunching the electron cloud does not appear (smooth bunch shape), nevertheless, exists some number of electrons. After the beam becomes coasting, a microbunch structure appears (which became severe for high intensity beams and eventually disappear

when the beam is totally unbunched), then, if the multipactor condition is reached, the number of electron increases and the electron cloud occurs. In Figs. 4 and 5 only the higher intensities presented a significant increase of the electron signal with respect to the early stage, therefore, in these cases the electron cloud occurred. Thus, the simulations results are consistent with the measurements.

Finally, Fig. 6 presents a remarkable enhancement of the electron generation for the sinusoidal frequency in the range of 20 to 50 MHz, this result is in agreement with the frequency bounce observed by the the electron cloud detector and the fast current transformer monitor in the cases with electron cloud [6].

REFERENCES

[1] K. Ohmi et al., Phys. Rev. ST Accel. Beams 5, 114402 (2002).

[2] T. Toyama et al., "Electron Cloud Effects in the J-PARC Rings and Related Topics", Proceedings of ECLOUD Vol. 4 (2004).

[3] K. Ohmi et al., "Study of EP Instability for a Coasting Proton Beam in Circular Accelerators", in Proceedings of the Particle Accelerator Conference, 2003, pp. 3083–3085.

[4] M. Tomizawa et al., "Injection and Extraction Orbit of the J-PARC Main Ring", Proceedings of European Particle Accelerator Conference 06 (2006).

[5] M. Uota et al., "Observation of Electron Cloud in J-PARC Main Ring", in Proceedings of the 9th Particle Accelerator Society of Japan, Osaka, Japan, August 8 - 11, 2012, pp. 462–465.

[6] B. Yee-Rendon et al., "Electron Cloud Measurements at J-PARC Main Ring", in Proceedings of the 7th International Particle Accelerator Conference, Busan, Korea, May 8 - 13, 2016, pp. 4175–4177.

[7] B. Yee-Rendon et al., "Electron Cloud Study at SX Operation Mode at J-PARC MR", in Proceedings of the 13th Particle Accelerator Society of Japan, Chiba, Japan, August 8 - 10, 2016, pp. 149–151.

[8] T. Toyama, private communication.

[9] M. Okada et al., "Control of the Multipactoring by the Surface Coating of the Exciter Electrodes in J-PARC MR", in Proceedings of the 7th Particle Accelerator Society of Japan (2010).